MALAYSIAN JOURNAL OF ANALYTICAL SCIENCES

Journal homepage: https://mjas.analis.com.my/

Research Article

Comparative study of *Hibiscus rosa-sinensis* and *Azadirachta indica* leaf extracts as efficient green corrosion inhibitors for mild steel in 1M HCl

Mohd Lias Kamal[1*], Farah Hanis Hamid[1], Shahrizal Hasan[1] and Khairil Anuar Jantan[2*]

[1]Faculty of Applied Sciences, Universiti Teknologi MARA, Perlis Branch, 02600, Arau, Perlis, Malaysia
[2]School of Chemistry and Environment, Faculty of Applied Sciences, Universiti Teknologi MARA, 40450 Shah Alam, Selangor, Malaysia

[*]Corresponding author: e-mail: mohdlias@uitm.edu.my and khairil0323@uitm.edu.my

Received: 3 September 2025; Revised: 12 December 2025; Accepted: 5 January 2026; Published: 28 February 2026

Abstract

This study established *Hibiscus rosa-sinensis* (HRS) leaf extract as a highly superior green corrosion inhibitor for mild steel in 1 M HCl, directly outperforming *Azadirachta indica* (Neem). Through a multi-methodological approach, the study demonstrated that both ethanolic extracts served as effective mixed-type inhibitors, with efficiency scaling with concentration. At an optimal concentration of 400 ppm, HRS achieved exceptional inhibition efficiencies of 92%—96%, significantly surpassing the 87%—91% range shown by Neema cross electrochemical and gravimetric evaluations. FTIR-ATR analysis confirmed the presence of rich concentrations of flavonoids and polyphenolics in both extracts, with the superior performance of HRS attributed to its enhanced adsorption capability and the formation of a more robust protective film, a mechanism unequivocally validated by SEM surface analysis. These findings not only provided a definitive comparative assessment, but also positioned HRS leaf extract as an outstanding, eco-friendly alternative for industrial corrosion mitigation in acidic environments.

Keywords: corrosion inhibitor, mild steel, hydrochloric acid, *Hibiscus rosa-sinensis*, *Azadirachta indica*

Introduction

Mild steel is the undisputed backbone of global industry; a material prized for its strength, malleability and low cost [1,2]. It forges our structural frameworks [3], pipelines [4], storage tanks [5] and machinery [6]. Yet, this versatility carries a critical vulnerability: a relentless susceptibility to corrosion [7,8]. In aggressive environments, this decay inflicts massive economic losses and elevates safety risks. This threat intensifies during pickling, an essential pre-treatment, whereby acidic solutions strip steel of mill scale and rust [9]. Hydrochloric acid (HCl) is the prime choice of industry, lauded for its potent descaling power and operational ease [10]. But, HCl is a double-edged sword; it cleanses the surface while ruthlessly attacks the steel beneath. To curb this destruction, corrosion inhibitors are not only beneficial but also indispensable [11,12]. These additives form a protective shield on the metal, significantly slowing the corrosive effect of the acid.

Traditionally, inorganic inhibitors [13] and synthetic organic compounds [14] have been deployed for this purpose. Their effectiveness is often attributed to functional groups with heteroatoms (N, O, S, P) and π-electrons, which facilitate adsorption onto the metal surface [15]. However, the majority of these conventional inhibitors are now heavily restricted or obsolete due to their pronounced toxicity, high environmental persistence and non-biodegradability, raising serious ecological and health concerns [16]. This has catalysed a paradigm shift within the field towards the development of environmentally benign, non-toxic and sustainable alternatives, collectively referred to as “green corrosion inhibitors” [17].

Plant extracts have surged to the forefront of this movement. They are abundant, renewable and economically compelling [18]. Their power derives from a sophisticated cocktail of natural phytochemicals, including alkaloids, flavonoids, tannins and terpenoids, all of which are rich in the very heteroatoms that enable potent metal adsorption [19,20]. Utilising these extracts converts waste biomass into a valuable resource, aligning perfectly with the principles of green chemistry. Two standout candidates, ubiquitous in Southeast Asia, are *Azadirachta indica* (Neem) and *Hibiscus rosa-*

sinensis (Hibiscus). Both are ethnopharmacological treasures, renowned for their bioactive and antioxidant-rich profiles [21,22]. Hibiscus leaves boast significant flavonoids, tannins, and saponins [23]; Neem delivers potent azadirachtin, gedunin and quercetin [24]. Their molecular architectures promise strong metal adsorption. While each has been studied in isolation, a critical gap remains: a definitive, head-to-head comparative study that deciphers the structure-performance relationship behind their efficacy.

Therefore, this study bridges the gap by comparing the effects of HRS and Neem leaf extracts as green corrosion inhibitors for mild steel in 1.0 M HCl. The investigation combines gravimetric analysis, electrochemical techniques (potentiodynamic polarisation and impedance spectroscopy), FTIR spectroscopy and surface morphology examination to assess their inhibition performance and mechanism comprehensively.

Materials and Methods

Materials and reagents

Fresh HRS leaves and Neem leaves were harvested in Perlis, Malaysia (6.5170° N, 100.2152° E). Analytical grade hydrochloric acid (HCl, 37%) and absolute ethanol (96%) were used as received from Merck. All solutions were prepared by using distilled water. The mild steel coupons were fabricated from AISI 1040 grade steel with a composition (wt.%) of 0.40% C, 0.75% Mn, 0.04% P, 0.05% S and the remainder Fe.

Preparation of steel specimens

The steel specimens were prepared in two geometries: for weight-loss tests, square coupons (1.0 cm × 1.0 cm × 0.1 cm) were cut, and a small hole (~2 mm) was drilled for suspension. For electrochemical tests, rectangular specimens (2.0 cm × 0.5 cm × 0.15 cm) were cut to fit the electrode holder. All specimens were subsequently ground sequentially with silicon carbide (SiC) abrasive paper up to 1200 grit, rinsed thoroughly with distilled water, degreased with absolute ethanol, dried in warm air, and stored in a desiccator before use. The final prepared surface was mirror-smooth to ensure consistency [25].

Preparation of inhibitor extracts

The inhibitor extracts were prepared using standard maceration techniques. The collected leaves were washed with distilled water to remove dust and impurities, air-dried for three weeks in a shaded, well-ventilated area, and then pulverized into a fine powder using a mechanical grinder. For each plant, 100 g of the dried leaf powder was immersed in 1000 mL of 96% ethanol in a sealed glass container and agitated periodically for 72 hours at room temperature. The resulting mixture was first filtered through coarse filter paper and then through fine filter paper (Whatman No. 1) to separate the solid residue. The ethanolic filtrate was concentrated using a rotary evaporator (Heidolph, Germany) at 50 °C under reduced pressure to obtain a crude paste. This paste was further dried in an oven at 60 °C for 24 hours to yield a solid extract. The extract was stored in a sealed container at 4 °C. Stock solutions of the inhibitors (1000 ppm) were prepared by dissolving 100 mg of the solid extract in 100 mL of 1.0 M hydrochloric acid (HCl). The test solutions with the desired concentrations (100, 200, 300, and 400 ppm) were prepared by diluting the stock solution with the acid medium to the appropriate concentration [26].

Electrolyte preparation

A corrosive electrolyte of 1.0 M HCl was prepared by diluting 83.3 mL of concentrated HCl (37%) to 1000 mL with distilled water in a volumetric flask. The concentration was verified by titration with a standard sodium carbonate solution.

Gravimetric (weight-loss) measurements

Gravimetric experiments were conducted by immersing the pre-weighed steel coupons in 100 ml of the test solutions (blank 1.0 M HCl and HCl with various inhibitor concentrations) for 168 h (7 days) at room temperature (28 ± 1 °C). The tests were performed in triplicate to ensure reproducibility. Percentage inhibition efficiency (IE%) was calculated by using the following equation [27]:

$$IE\% = \frac{W - W_i}{W} \times 100 \quad (1)$$

where, w is weight loss without inhibitor (0 ppm), and W_i is weight loss with inhibitor (100 ppm, 200 ppm, 300 ppm, 400 ppm). The surface coverage area ($\boldsymbol{\theta}$) was estimated by the subsequent equation:

$$\boldsymbol{\theta} = \frac{IE(\%)}{100} \quad (2)$$

Electrochemical measurements

All electrochemical experiments were performed by using an Autolab PGSTAT302N potentiostat/ galvanostat (Metrohm, Netherlands) controlled by Nova 2.1 software. A conventional three-electrode glass cell was used, which comprised an AISI 1040 steel working electrode, a platinum (Pt) counter electrode and a silver/silver chloride (Ag/AgCl) reference electrode. Prior to each measurement, the working electrode was immersed in the test solution for 30 min to establish a stable open-circuit potential (OCP). Electrochemical impedance spectroscopy (EIS) measurements were conducted at the OCP in the frequency range from 100 kHz to 10 mHz with an applied AC amplitude of 10 mV. The impedance data were fitted to appropriate equivalent circuits by using Nova software.

Potentiodynamic polarisation (PDP) curves were recorded immediately after EIS by scanning the potential from -250 mV to +250 mV vs. OCP at a scan rate of 1 mV/s. Corrosion current density (i_{corr}) was determined by using the Tafel extrapolation method. All experiments were conducted at room temperature and repeated at least twice to verify consistency. Inhibition efficiencies from PDP (IE%) and EIS (IE%) were calculated by using the following equations.

$$IE\% = \frac{(I'_{corr}) - (I_{corr})}{(I'_{corr})} \times 100 \quad (3)$$

where I'_{corr} and I_{corr} are the corrosion currents in the absence and presence of the inhibitor.

$$IE\% = \frac{(R'_{ct}) - (R_{ct})}{(R'_{ct})} \times 100 \quad (4)$$

where R_{ct} and R'_{ct} are the corrosion currents without and with the green corrosion inhibitor [28].

Surface characterization

The functional groups present in the solid inhibitor extracts were characterised by using a Perkin Elmer Spectrum 1600 FTIR spectrometer equipped with an attenuated total reflectance (ATR) accessory. Spectra were recorded in the range of 4000 cm^{-1}–400 cm^{-1}. The surface morphology of mild steel specimens after 24 h of immersion in blank 1.0 M HCl and in HCl containing 400 ppm of each inhibitor was examined by using a Hitachi tabletop microscope TM3030. The samples were prepared for weight-loss test, dried and directly imaged without further coating to observe the topographical changes resulting from corrosion and inhibitor adsorption.

Results and Discussion

Inhibition efficiency by gravimetric analysis

Gravimetric assessment following 168 h of immersion in 1.0 M HCl revealed a substantial corrosion of mild steel in the uninhibited solution, with mass loss of 0.5717 g. The introduction of plant extracts markedly attenuated corrosive degradation, even at the lowest concentration of 100 ppm, indicating prompt adsorption of inhibitory compounds onto the metal substrate. A concentration-dependent amelioration in corrosion inhibition was observed for both leaf extracts. Inhibition efficiency (IE%) increased progressively with elevated concentration, consistent with enhanced surface coverage (θ) as adsorption sites became occupied by inhibitor molecules, which is a behaviour characteristic of effective interfacial inhibition [29]. Maximum efficacy was attained at 400 ppm, which was the highest concentration evaluated (**Table 1**).

At this maximum concentration, HRS leaf extract exhibited superior performance, achieving an inhibition efficiency of 93.79% (θ = 0.9379), indicating near-complete surface coverage and the formation of a protective film that markedly impeded acid attack. Neem leaf extract also demonstrated significant inhibitory activity, attaining an IE of 89.87% (θ = 0.8987) under identical conditions. Comparative analysis unequivocally established the enhanced performance of HRS across all concentrations, with a statistically significant advantage of approximately four percentage points at 400 ppm. This disparity in efficacy was substantively relevant for industrial applications and was likely attributable to differential phytochemical composition, molecular architecture and adsorption energetics of the respective extracts. The elevated IE and θ values suggested a stronger affinity of HRS constituents for the mild steel surface, potentially due to a higher density of functional groups, propensity for chemisorption or synergistic interactions amongst bioactive compounds [30].

Table 1. IE of HRS and Neem extracts for various concentrations against MS in 1M HCl at room temperature by weight loss measurement

	Concentration (ppm)	Initial Weight (g)	End weight (g)	Weight Difference (g)	θ	IE (%)
HCl	1M	0.9074	0.3857	0.5717	-	-
Hibiscus rosa-sinensis	100	0.9076	0.6982	0.2094	0.6337	63.37
	200	0.9082	0.7928	0.1154	0.7982	79.82
	300	0.9089	0.8452	0.0637	0.8886	88.86
	400	0.9079	0.8724	0.0355	0.9379	93.79
Azadirachta indica	100	0.9081	0.6667	0.2414	0.5776	57.76
	200	0.9057	0.8331	0.0726	0.8730	87.30
	300	0.9089	0.8453	0.0636	0.8888	88.88
	400	0.9081	0.8502	0.0579	0.8987	89.87

Furthermore, the sustained high inhibition efficiencies (>89%) over the extended immersion period (168 h) underscored not only the effectiveness, but also the remarkable stability of the inhibitor films. The persistence of inhibitory performance indicated robust adsorption and resistance to desorption or degradation within the acidic medium, a critical attribute for the practical implementation of industrial acidising processes.

Potentiodynamic polarization

Potentiodynamic polarisation measurements were employed to elucidate the kinetic parameters and inhibition mechanism of the plant extracts. The polarisation curves (**Figure 1**) and corresponding parameters (**Table 2**) provided substantial insight into the inhibitory effects on both anodic and cathodic reactions governing the corrosion of mild steel in 1.0 M HCl. The polarisation behaviour demonstrated significant inhibition, as evidenced by pronounced cathodic shifts and a substantial reduction in current density. The uninhibited 1 M HCl solution exhibited the highest corrosion current density, I_{corr} (90.60 µA cm^{-2}), indicating rapid corrosion kinetics. The systematic addition of both leaf extracts resulted in concentration-dependent suppression of both anodic and cathodic branches, as evidenced by a displacement towards lower current densities [31]. This effect culminated at 400 ppm, whereby HRS and Neem reduced the corrosion current density to 3.89 µA cm^{-2} and 8.49 µA cm^{-2}, corresponding to inhibition efficiencies of 95.71% and 90.63%, respectively. The order-of-magnitude reduction in corrosion rate underscored the substantial efficacy of both extracts, with HRS demonstrating superior performance.

Polarisation curves in **Figure 1** were paramount for classifying the inhibition mechanism. The inhibition mechanism was classified through analysis of corrosion potential (E_{corr}) shifts. For both inhibitors, the maximal displacement of E_{corr} was less than 11 mV relative to the blank, which was below the 85 mV threshold established for classifying inhibitor type [32]. This minimal displacement, coupled with concurrent suppression of both anodic and cathodic reactions, confirmed mixed-type inhibition behaviour. The results indicated that adsorbed phytochemical constituents formed a protective barrier that impeded both metal dissolution (anodic reaction: $Fe \rightarrow Fe^{2+} + 2e^-$) and hydrogen evolution (cathodic reaction: $2H^+ + 2e^- \rightarrow H_2$), rather than selectively altered either half-cell reaction.

Further mechanistic insight was gained from analysis of Tafel slopes (β_a *and* β_c) in **Table 2**. The alterations in both anodic and cathodic slopes upon inhibitor addition indicated modifications to the mechanisms of both partial reactions [33]. Notably, HRS at 400 ppm induced a substantial decrease in both βa and βc values (to 28.83 and 29.36 mV/dec, respectively), suggesting the formation of a highly effective protective film that transitions the corrosion process towards diffusion-controlled kinetics. The symmetrical shaping of the polarisation curves at this concentration further supports the development of a robust inhibitory layer.

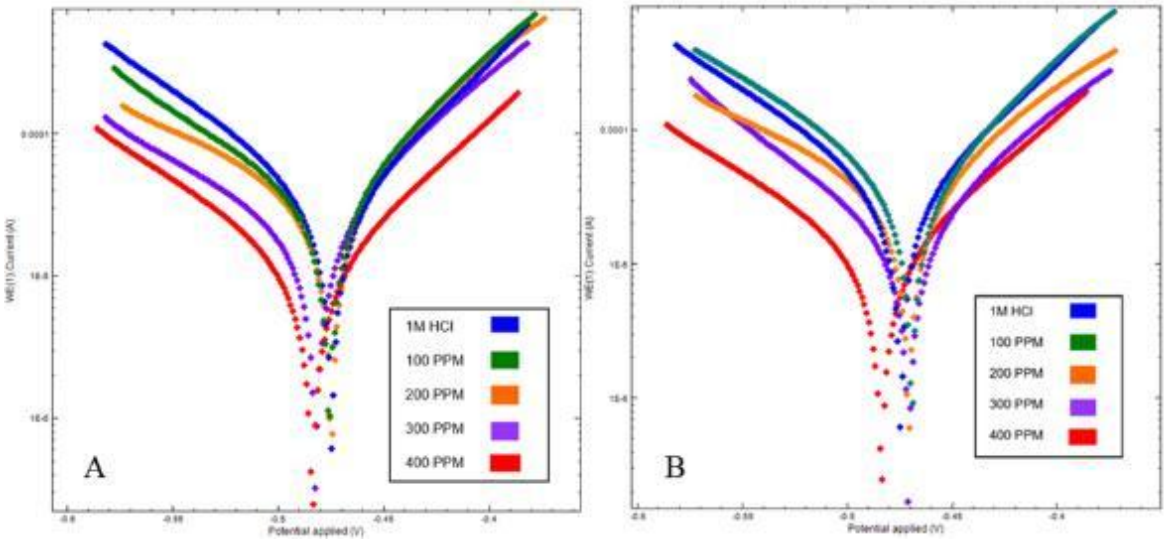

Figure 1. Tafel polarisation curves for mild steel in 1 M HCl in the absence and presence of different concentrations of (A) HRS extract and (B) Neem extracts

Table 2. Potentiodynamic polarisation for HRS and Neem at selected concentrations in 1M HCl at room temperature

	Concentration (ppm)	Tafel Slopes (mV vs. dec)		-E_{corr} (mV)	I_{corr} (μAcm^{-2})	IE (%)
		β_a	β_c			
HCl	1M	256.77	192.88	474.59	90.60	-
Hibiscus rosa-sinensis	100	150.13	84.56	479.69	44.19	51.23
	200	149.59	73.37	469.91	35.65	60.65
	300	168.55	75.42	477.76	25.24	72.14
	400	28.83	29.36	484.65	3.89	95.71
Azadirachta indica	100	105.02	90.28	477.72	43.81	51.64
	200	137.65	85.08	470.73	35.91	60.36
	300	185.05	78.68	478.87	26.84	70.38
	400	62.95	62.91	485.05	8.49	90.63

Table 3. Impedance parameters for HRS and Neem at selected concentrations in 1M HCl at room temperature

	Concentration (ppm)	R_{ct} ($\Omega \cdot cm^2$)	C_{dl} ($\mu F.cm^2$)	IE (%)
HCl	1M	12.5	636.6	-
Hibiscus rosa-sinensis	100	37.3	533.7	66.5
	200	71.1	640.1	82.4
	300	108.8	731.3	88.5
	400	157.3	1012.6	92.1
Azadirachta indica	100	27.5	482.3	54.5
	200	78.9	532.3	84.2
	300	86.2	578.1	85.5
	400	93.6	680.3	86.6

In conclusion, the potentiodynamic polarisation analysis unequivocally demonstrated that these plant extracts were effective inhibitors of mixed-type corrosion. The concentration-dependent efficacy and high inhibition efficiencies at maximum concentration (400 ppm) established these plant extracts as promising green alternatives to conventional toxic inhibitors for acid corrosion protection.

Electrochemical Impedance Spectroscopy (EIS)

Electrochemical impedance spectroscopy (EIS) provided further insight into the kinetics and mechanism of the corrosion inhibition process. The most salient feature of the EIS data was the significant increase in charge transfer resistance (R_{ct}) upon addition of the plant extracts. The R_{ct} value, obtained from the diameter of the capacitive loop, was a direct measure of the electron transfer resistance across the metal-solution interface and was inversely proportional to the corrosion rate [34]. The R_{ct} value for the uninhibited 1 M HCl solution was 12.5 $\Omega \cdot cm^2$. This value increased markedly with the addition of inhibitors, in a concentration-dependent manner. Notably, at the optimal concentration of 400 ppm, HRS exhibited a maximum R_{ct} of 157.3 $\Omega \cdot cm^2$, while Neem reached 93.6 $\Omega \cdot cm^2$. This substantial increase in R_{ct} quantitatively confirmed the formation of a highly resistive film on the mild steel surface that effectively impedes the charge transfer processes necessary for corrosion [35].

Inhibition efficiency (IE%) corroborated the trends observed from gravimetric and polarisation studies. The efficiencies increased with concentration, reaching a maximum of 92.1% and 86.6% for HRS and Neem, respectively, at 400 ppm. The consistently higher IE% and *Rct* values for HRS across all concentrations reaffirmed its superior protective capability as compared to Neem. Analysis of the double-layer capacitance (*Cdl*) offered crucial information on the interfacial changes. The C_{dl} values were calculated from the frequency at the maximum imaginary impedance (f_{max}) by using the following formula [35]:

$$C_{dl} = \frac{1}{2\pi f_{max}} \times \frac{1}{R_{ct}} \quad (5)$$

where, f_{max} is maximum frequency at which the imaginary component of Nyquist plot is maximum

Value for the blank solution was 636.6 μF·cm^{-2}. Addition of the inhibitors generally caused a decrease in *Cdl*, as seen for Neem, which dropped to 482.3 μF·cm^{-2} at 100 ppm. This decrease was a classic indicator of successful inhibitor adsorption and could be explained by the Helmholtz model [36]. The occasional slight increase in *Cdl* for some concentrations of HRS was not uncommon in inhibitor studies and might be attributed to a localised increase in surface roughness or a change in the electroactive area due to the specific adsorption mode of its complex phytochemical constituents [21]. However, the overarching trend, especially the significant rise in *Rct*, remains the primary evidence for effective inhibition. The Nyquist plots (**Figure 2**) typically exhibited depressed, single capacitive loops, which were characteristic of charge-transfer-controlled processes on electrochemically heterogeneous surfaces. The increased diameter of these loops with inhibitor concentration provided visual confirmation of the enhanced corrosion resistance.

FTIR analysis of green inhibitors

Fourier transform infrared (FTIR) spectroscopy was employed to characterise the functional groups present in the HRS leaf extract and Neem leaf extract and to elucidate the molecular basis for their corrosion inhibition properties. The spectra for both leaf extracts are presented in **Figure 3**, revealing a complex profile of bioactive constituents that were instrumental in the adsorption process. The FTIR analysis confirmed the presence of several key functional groups characteristic of potent corrosion-inhibiting compounds. A broad and intense absorption band observed at approximately 3340 cm^{-1} for HRS and 3318 cm^{-1} for Neem was unequivocally assigned to the O-H stretching vibration of phenolic compounds and water [26]. The broad nature of this band was indicative of strong hydrogen bonding, a property that can facilitate interaction with the hydrated metal surface.

A critical diagnostic band for flavonoids and other polar organic molecules, the strong C=O stretching vibration of the carbonyl group, was identified at 1722 cm^{-1} and 1707 cm^{-1} for HRS leaf extract and Neem extract, respectively. The presence of conjugated carbon-carbon double bonds (C=C), a hallmark of aromatic rings in polyphenolic structures, was confirmed by sharp peaks at 1628 cm^{-1} (HRS) and 1608 cm^{-1} (Neem). Further evidence for aromatic systems was provided by the peaks at approximately 1438 cm^{-1}, attributable to aromatic C-H in-plane bending vibrations. Additionally, the aliphatic C-H stretching vibrations observed around 2922 cm^{-1} in the Neem extract were consistent with the methyl and methylene groups prevalent in terpenoid structures, such as azadirachtin, one of its primary active components [37,38].

Surface morphology

Scanning electron microscopy (SEM) was employed to provide direct visual evidence of the protective effect afforded by the HRS extract and Neem extracts on the mild steel surface. The micrographs, presented in **Figure 4**, offered a stark morphological contrast which corroborated the electrochemical and gravimetric findings. Surface of the mild steel specimen exposed to the uninhibited 1 M HCl solution (**Figure 4A**) exhibited severe deterioration, characterised by a rough, porous and heavily etched morphology. This extensive damage was a direct consequence of aggressive acid attack, resulting in uniform corrosion and significant metal dissolution over the 24-hour immersion period.

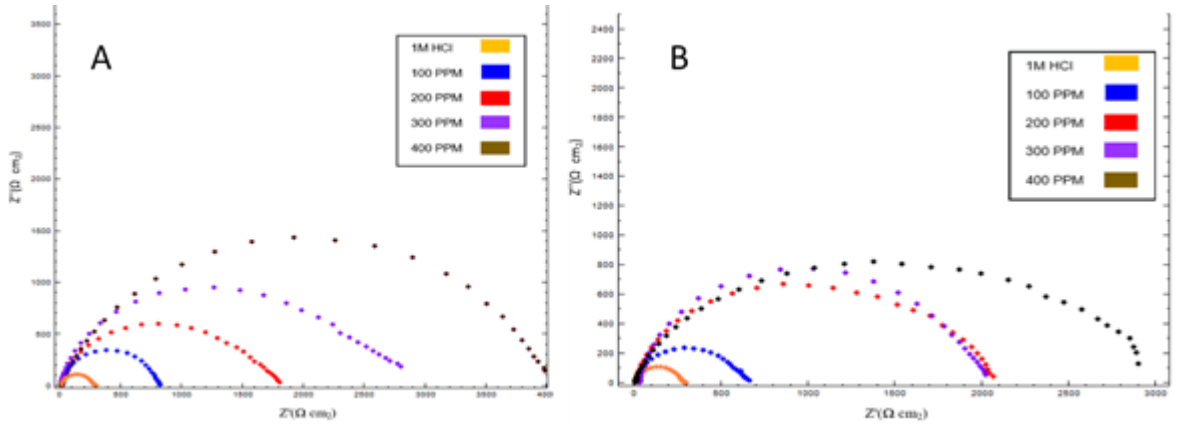

Figure 2. Impedance for MS specimen in 1M HCl with and without various concentrations of HRS leaf extract (A) and Neem leaf extract (B)

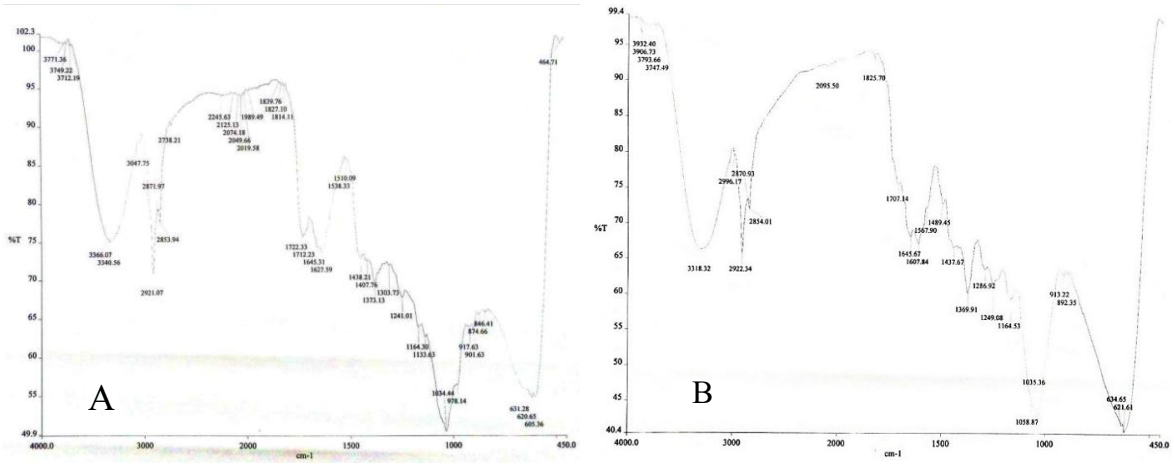

Figure 3. FTIR spectra of HRS extract (A) and Neem (B) extract

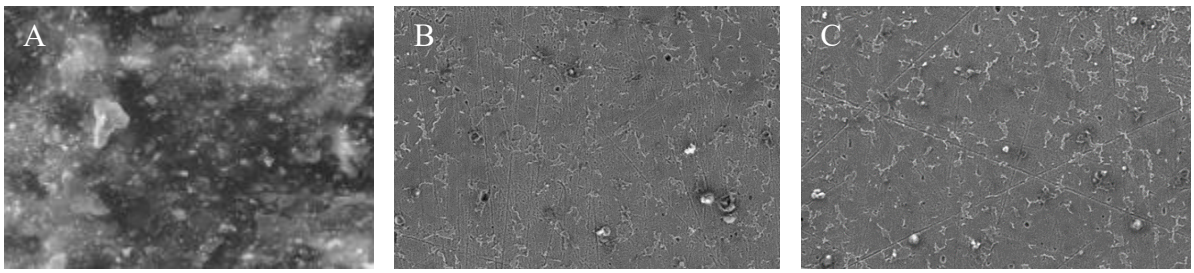

Figure 4. SEM images of MS: (A) absence of inhibitor, and presence of HRS (B) extract and Neem (C) extract

In profound contrast, the surfaces of specimens protected with 400 ppm of the plant extracts (**Figure 4B, 4C)** remained remarkably intact and smooth. The micrograph for the surface inhibited by HRS (Figure 4B) showed only minor, superficial etching, while the surface protected by Neem (**Figure 4C**) also demonstrated significant improvement as compared to the blank, though with slightly more visible surface features. This dramatic improvement in surface morphology is a direct result of the adsorption of inhibitor molecules, which formed a coherent protective layer that acted as a barrier, shielding the underlying metal from direct contact with the corrosive electrolyte [39].

The correlation between surface morphology and quantitative performance was clear. The superior surface smoothness observed for the HRS-protected sample aligned perfectly with its higher inhibition efficiency (92.1%) as compared to Neem(86.6%) and was determined by electrochemical techniques. Therefore, the SEM evidence provided incontrovertible visual proof of the proposed inhibition mechanism, confirming that the bioactive compounds in both extracts adsorb onto the mild steel surface to form a compelling protective film that significantly mitigated acid-induced corrosion.

Conclusion

This study establishes ethanolic extracts of HRS and Neem as effective green corrosion inhibitors for mild steel in 1 M HCl. Exhibiting mixed-type inhibition, the extracts achieved efficiencies of 92.1% and 86.6%, respectively, at 400 ppm. HRS demonstrated superior performance due to enhanced adsorption and robust protective film formation, facilitated by electron-donating flavonoids and polyphenolics. The mechanism was validated electrochemically, with FTIR confirming active adsorption sites and SEM visualising surface protection. These findings positioned HRS as a promising sustainable alternative to conventional inhibitors for industrial acid applications.

Acknowledgment

The authors express their sincere thanks to the Faculty of Applied Sciences at UiTM Perlis and Shah Alam for their significant support and the provision of research facilities. K.A.J. is particularly grateful to the Ministry of Higher Education, Malaysia, and Universiti Teknologi MARA for their generous support and funding through a scholarship under the Post-Doctoral Training Scheme (grant code: KPT(BS)820710105709).

References

1. Birat, J. P. (2020). Society, materials, and the environment: The case of steel. *Metals*, 10(3), 331.
2. Hernandez, A. G., Paoli, L., & Cullen, J. M. (2018). How resource-efficient is the global steel industry?. *Resources, Conservation and Recycling*, 133, 132-145.
3. Raabe, D., Tasan, C. C., & Olivetti, E. A. (2019). Strategies for improving the sustainability of structural metals. *Nature*, 575(7781), 64-74.
4. Parlak, B. O., & Yavasoglu, H. A. (2023). A comprehensive analysis of in-line inspection tools and technologies for steel oil and gas pipelines. *Sustainability*, *15*(3), 2783.
5. Cheng, Q., Zhang, R., Shi, Z., & Lin, J. (2024). Review of common hydrogen storage tanks and current manufacturing methods for aluminium alloy tank liners. *International Journal of Lightweight Materials and Manufacture*, 7(2), 269-284.
6. Ishfaq, K., Anjum, I., Pruncu, C. I., Amjad, M., Kumar, M. S., & Maqsood, M. A. (2021). Progressing towards sustainable machining of steels: a detailed review. *Materials*, 14(18), 5162.
7. Manu, K. C., Madhushree, C., Chandini, M. S., Shree, N., Hemanth, S., & Jeevan, T. P. (2025). Corrosion in Steel Structures: A Review. *Journal of Mines, Metals & Fuels*, *73*(1), 10.
8. Aljibori, H. S., Alamiery, A., & Kadhum, A. A. H. (2023). Advances in corrosion protection coatings: A comprehensive review. *International Journal Corrosion Scale Inhibition*, 12(4), 1476-1520.
9. Choudhury, A. R., Singh, N., Veeraraghavan, A., Gupta, A., Palani, S. G., Mehdizadeh, M., & Al-Taey, D. K. (2023). Ascertaining and optimizing the water footprint and sludge management practice in steel industries. *Water*, 15(12), 2177.
10. Almubarak, T., Ng, J. H., Ramanathan, R., & Nasr-El-Din, H. A. (2022). From initial treatment design to final disposal of chelating agents: a review of corrosion and degradation mechanisms. *RSC advances*, 12(3), 1813-1833.
11. Chen, L., Lu, D., & Zhang, Y. (2022). Organic compounds as corrosion inhibitors for carbon steel in HCl solution: a comprehensive review. *Materials*, 15(6), 2023.
12. Răuță, D. I., Matei, E., & Avramescu, S. M. (2025). Recent development of corrosion inhibitors: types, mechanisms, electrochemical behavior, efficiency, and environmental impact. *Technologies*, *13*(3), 103.
13. Al-Amiery, A. A., Yousif, E., Isahak, W. N. R. W., & Al-Azzawi, W. K. (2023). A review of inorganic corrosion inhibitors: types, mechanisms, and applications. *Tribology in Industry*, 44(2), 313.
14. Al-Amiery, A. A., Isahak, W. N. R. W., & Al-Azzawi, W. K. (2023). Corrosion inhibitors: natural and synthetic organic inhibitors. *Lubricants*, 11(4), 174.
15. Ahmed, M. A., Amin, S., & Mohamed, A. A. (2024). Current and emerging trends of inorganic, organic and eco-friendly corrosion inhibitors. *RSC Advances*, 14(43), 31877-31920.
16. Njoku, C. N., Maduoma, T. U., Emori, W., Odey, R. E., Unimke, B. M., Yakubu, E., ... & Oyoh, K. B. (2024). Natural and synthetic drugs as eco-friendly and sustainable corrosion inhibitors for metals: A review. *Pigment & Resin Technology*, 53(6), 1074-1087.
17. Popoola, L. T. (2019). Organic green corrosion inhibitors (OGCIs): A critical review. *Corrosion Reviews*, 37(2), 71-102.
18. Marzorati, S., Verotta, L., & Trasatti, S. P. (2018). Green corrosion inhibitors from natural sources and biomass wastes. *Molecules*, 24(1), 48.
19. Gautam, P., Saurav, & Shankar, J. (2025). Exploring green inhibitors from microbes and plants: Current trends and future perspectives in sustainable approach. *Journal of Bio-and Tribo-Corrosion*, *11*(2), 56.
20. Verma, C., Alfantazi, A., Quraishi, M. A., & Rhee, K. Y. (2023). Are extracts really green substitutes for traditional toxic corrosion inhibitors? Challenges beyond origin and availability. *Sustainable Chemistry and Pharmacy*, 31, 100943.
21. Amtaghri, S., Qabouche, A., Slaoui, M., & Eddouks, M. (2024). A comprehensive overview of Hibiscus rosa-sinensis L.: Its ethnobotanical uses, phytochemistry, therapeutic uses, pharmacological activities, and toxicology. *Endocrine, Metabolic & Immune Disorders-Drug Targets (Formerly Current Drug Targets-Immune, Endocrine & Metabolic Disorders)*, 24(1), 86-115.
22. Sarkar, S., Singh, R. P., & Bhattacharya, G. (2021). Exploring the role of Azadirachta indica (neem) and its active compounds in the regulation of biological pathways: an update on molecular approach. *3 Biotech*, *11*(4), 178.
23. Udo, I. J., Ben, M. G., Etuk, C. U., & Tiomthy, A. I. (2016). Phytochemical, proximate and antibacterial properties of Hibiscus rosa-sinensis L. Leaf. *Journal of Medicinal Plants Studies*, 4(5), 193-195.
24. Devi, J., & Sharma, R. B. (2023). Medicinal importance of Azadirachta indica: An overview. *J. Drug Deliv. Therap*, 13(6), 159-165.
25. Rodda, J. R., & Ives, M. B. (2003). Determination of corrosion rates in hot, concentrated sulfuric acid. *Corrosion*, 59(4), 363-370.
26. Prasanna, R., Manonmani, P., Elangomathavan, R., & Goel, M. (2018). Anti corrosion studies on ethanolic extract of Hibiscus Rosa sinensis and azadirachita Indica leaves. *International Journal Civil Engineering Technology*, 9, 219-229.

27. Mourya, P., Banerjee, S., & Singh, M. M. (2014). Corrosion inhibition of mild steel in acidic solution by Tagetes erecta (Marigold flower) extract as a green inhibitor. *Corrosion Science*, 85, 352-363.
28. Kurniawan, F., & Madurani, K. A. (2015). Electrochemical and optical microscopy study of red pepper seed oil corrosion inhibition by self-assembled monolayers (SAM) on 304 SS. *Progress in Organic Coatings*, 88, 256-262.
29. Sabiha, M., Kerroum, Y., El Hawary, M., Boudalia, M., Bellaouchou, A., Hammani, O., & Amin, H. M. (2025). Investigating the adsorption and corrosion protection efficacy and mechanism of marjoram extract on mild steel in HCl medium. *Molecules*, 30(2), 272.
30. Oguzie, E. E. (2008). Corrosion inhibitive effect and adsorption behaviour of Hibiscus sabdariffa extract on mild steel in acidic media. *Portugaliae Electrochimica Acta*, 26(3), 303-314.
31. Alvarez, P. E., Fiori-Bimbi, M. V., Neske, A., Brandán, S. A., & Gervasi, C. A. (2018). Rollinia occidentalis extract as green corrosion inhibitor for carbon steel in HCl solution. *Journal of Industrial and Engineering Chemistry*, 58, 92-99.
32. Holla, B. R., Mahesh, R., Manjunath, H. R., & Anjanapura, V. R. (2024). Plant extracts as green corrosion inhibitors for different kinds of steel: A review. *Heliyon*, 10(14), e33748.
33. Shanmugapriya, R., Ravi, M., Ravi, S., Ramasamy, M., & Maruthapillai, A. (2023). Electrochemical and morphological investigations of *Elettaria cardamomum* pod extract as a green corrosion inhibitor for mild steel corrosion in 1 N HCl. *Inorganic Chemistry Communications*, 154, 110958.
34. Hernández, H. H., Reynoso, A. M. R., Juan, C., González, T., & Morán, C. O. G. (2020). Electrochemical Impedance Spectroscopy (EIS): A review study of basic aspects of the corrosion mechanism applied to. *Electrochemical impedance spectroscopy*, 1. Intech Open Publication.
35. Bammou, L., Belkhaouda, M., Salghi, R., Benali, O., Zarrouk, A., Zarrok, H., & Hammouti, B. (2014). Corrosion inhibition of steel in sulfuric acidic solution by the *Chenopodium Ambrosioides* extracts. *Journal of the Association of Arab Universities for Basic and Applied Sciences*, 16, 83-90.
36. Ivanov, V. D. (2024). The Helmholtz model. *Journal of Solid State Electrochemistry*, 28(8), 2487-2493.
37. Anuradha, K., Vimala, R., Narayanasamy, B., Arockia Selvi, J., & Rajendran, S. (2007). Corrosion inhibition of carbon steel in low chloride media by an aqueous extract of Hibiscus rosa-sinensis Linn. *Chemical Engineering Communications*, 195(3), 352-366.
38. Eddy, N. O., & Mamza, P. A. P. (2009). Inhibitive and adsorption properties of ethanol extract of seeds and leaves of *Azadirachta indica* on the corrosion of mild steel in H_2SO_4. *Portugaliae Electrochimica Acta*, 27(4), 443-456.
39. Taghavikish, M., Dutta, N. K., & Roy Choudhury, N. (2017). Emerging corrosion inhibitors for interfacial coating. *Coatings*, 7(12), 217.